A Quantitative Approach to Applications of Electronic Energy Transfer (EET)

Lennart B.-Å. Johansson

Contents

Abstract In brief, the Förster theory (FT) of electronic energy transfer (EET) between/among fluorescent and non-fluorescent molecules is discussed.

Here the EFT concerns applications for quantitative studies of biomolecular systems, in particular lipid membranes and proteins. The EET may take place within pairs of chromophores, as well as within random or regularly ordered distributions of chromophores. Described and exemplified are also relations between experimental data and theories.

Discussed finally are suggestions that aim at further extending the applicability of the FT.

Keywords EET in regular aggregates · Electronic energy transfer (EET) within pairs · Förster's theory · Two-particle approximation

Abbreviations

DAET	Donor to acceptor energy transfer, also referred to as *hetero* FRET
DDEM	Donor–donor energy migration, also referred to as *homo* fluorescence resonance energy transfer (FRET)

L. B.-Å.Johansson (✉)
Department of Chemistry, Umeå University, Umeå, Sweden
e-mail: Lennart.B.Johansson@umu.se

R. Šachl, M. Amaro (eds.), *Fluorescence Spectroscopy and Microscopy in Biology*,
Springer Ser Fluoresc (2023) 20: 87–98, https://doi.org/10.1007/4243_2022_28,
Published online: 14 August 2022

EET Electronic energy transfer
FT Förster's theory
MC Monte Carlo

1 Background to Förster's Theory

Early in the twentieth century [1–3] experiments revealed that electronic energy might be transferred without transfer of matter of any kind, e.g. as in sensitised fluorescence in vapours. A detailed physical explanation was at first derived from quantum theory by Theodor Förster [4]. The theoretical treatment also covers similar phenomena observed among chromophoric/fluorescent molecules. Förster's explanation assumes *weak coupling* between electric transition dipole moments of electronically excited ($\widehat{\mu}_{\mathrm{D}}$) and non-excited ($\widehat{\mu}_{\mathrm{A}}$) species (cf. Fig. 1). Within this approach and by applying quantum mechanical time-dependent perturbation theory, Förster derived the rate constant of electronic transfer (ω) between an electronically excited molecule {i.e. the donor group (D)} and another compound being in its electronic ground state, named the acceptor (A). In fact, the process defines a specific fluorescence quenching process of an excited D-molecule, but unlike most other fluorescence quenching processes the rate of EET is rather simply related to experimental properties. The rate of transfer reads:

$$\omega = \frac{3}{2}\frac{1}{\tau_{\mathrm{D}}}\kappa^2\left[\frac{R}{R_0}\right]^6 \tag{1}$$

Here τ_{D} stands for the fluorescence lifetime of the donor in absence of acceptors. The distance between D and A is R, whereas the Förster radius (R_0) can be calculated

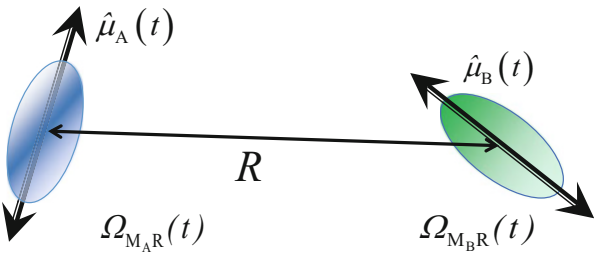

Fig. 1 Schematic indicating electric dipole–dipole coupling between two chromophoric molecules A and B. Here A and B denote the acceptor and B the donor, or both being donors, i.e. if A and B are of the same kind. The unit transition dipoles ($\widehat{\mu}_i, i = \mathrm{A}$ or B) are separated at a distance R with orientations described relative a common molecular frame of $\widehat{R}$, with mutual orientations indicated by Eulerian angles $\Omega_{M,R}$ ($i = \mathrm{A}$ or B). The time-dependence accounts for molecular reorientations that may change on the timescales of EET and fluorescence

from the overlapping between the corrected normalised D-fluorescence $\{f_D(\lambda)\}$ and molar absorptivity $\{\varepsilon_A(\lambda)\}$ spectra;

$$R_0 = \left\{ \frac{9000(\ln 10)(2/3)\Phi J}{125\pi^5 n^5 N_A} \right\}^{1/6} \tag{2a}$$

$$J = \int_{\text{spectra}} \varepsilon_A(\lambda) f_D(\lambda) \lambda^4 d\lambda \tag{2b}$$

Φ, n and N_A denote the fluorescence quantum yield of the donor, the refractive index of the solvent and the Avogadro constant, respectively. Conveniently, κ^2 is taken to be the isotropic average, i.e. $<\kappa^2> = 2/3$ for rotational motions being much faster than the transfer rates.

The κ^2-factor accounts for the mutual orientation of the coupled D and A electronic transition dipoles;

$$\kappa^2 = \left[\hat{\mu}_D \cdot \hat{\mu}_A - 3\left(\hat{\mu}_D \cdot \hat{R}\right)\left(\hat{R} \cdot \hat{\mu}_A\right) \right]^2 \tag{2c}$$

Here, $\hat{\mu}_A$, $\hat{\mu}_D$ and $\hat{R}$ denote unit vectors.

Notice that the above mechanism also explains energy transport between chromophoric molecules of the *same* kind, since their fluorescence and absorption spectra are usually overlapping. Thus, EET is possible from an excited D-molecule to another D molecule in its electronic ground state. We therefore have to distinguish between EET in two extreme cases, namely the reversible DD transfer and the irreversible DA transfer. The former process enables migration of the initially absorbed excitation energy among several donor molecules, i.e. between two or more donors and it is here referred to as a donor–donor energy migration (DDEM) in space.

From Förster's theory (i.e. Eqs. 1 and 2) it follows that spatial as well as orientational distributions can substantially influence the rate of EET.

2 Observing EET

Electronic energy transfer from an excited donor to an acceptor must shorten the D-fluorescence lifetime. It is therefore detectable by fluorescence lifetime measurements, or by the observed fluorescence spectral intensities, in presence and absence of acceptors. On the other hand, the reversible DD energy migration process implies that the number of excited donor molecules remains invariant, whereby the fluorescence relaxation time of donors remains equal to that in absence of coupling to ground-state donors. In most D-systems studied, however, the *mutual orientations* of a primary (or *initially*) and a secondarily excited D-molecule differ. Consequently the polarisation of the emitted fluorescent photon differs from that created by the

initially excited donors. The DDEM process obviously acts similar as to a reorientation of the primarily excited D. Fluorescence depolarisation experiments provide information about *changed* orientations of excited molecules at the times of excitation and fluorescence emission. Thus, depolarisation experiments simultaneously report on the rates of reorientations, as well as that of energy migrations among donors. Therefore, a fundamental question reads; how to distinguish between the two processes? A further elaboration on this is presented in subsections below.

2.1 Analyses of EET Data Within Pairs of Chromophores

Frequently applications of EET concern the determination of inter-chromophoric distances, e.g. as related to macromolecular structure. Numerous studies have been reported in the literature (see, e.g., the textbook of Lakowicz [5] and papers cited therein). Structural intramolecular distances within, e.g., a protein can be estimated in EET experiments by means of using DA or DD pairs. This, is because typical Förster radii range between ca. 10–100 Å, i.e. intramolecular distances in, as well as dimensions of proteins. A reasonable objection to the use of EET in this context would be that structural information is also available from NMR and X-ray studies, and these techniques often provide a higher resolution. However, this is *not* generally true, because these methods exhibit limitations for reasons of inherent restrictions, as well as difficulties in preparing samples. For instance, it has been shown that structural changes upon adequate perturbations/interactions are available from EET experiments on suitably labelled proteins [6, 7].

Pairs of chromophores could be naturally present (= commonly referred to as intrinsic probes), or artificially introduced (extrinsic probes) into a macromolecule. Well-defined extrinsic labelling of proteins is possible by means of *site-specific mutagenesis* for introducing reactive amino acids, which can be specifically labelled with reactive chromophores. For this purpose, Cys-residues are useful in the labelling of proteins with sulfhydryl specific chromophores. If no suitable intrinsic probes are available in a protein, it is most convenient to introduce two donor groups [7]. Hereby one avoids different mixtures of non-specific labelling of two reactive positions with possible combinations and fractions of D-A, A-D, D-D and A-A pairs.

The excitation probability of the *initially* excited D group within a DD or a DA pair at a time t later $\{\chi(t)\}$ is according to Förster's theory given by:

$$\chi(t) = \frac{1}{2}[1 + \exp(-\gamma\langle\omega\rangle t)]F_{\mathrm{D}}(t), \tag{3}$$

where $\gamma = 1$ or 2 for DA or DD transfer, respectively. The bracket $\langle\omega\rangle$ indicates an orientational average of the interacting electronic transition dipoles. Furthermore, $F_{\mathrm{D}}(t)$ denotes the fluorescence relaxation in the absence of EET.

As pointed out above only fluorescence depolarisation experiments reveal DD electronic energy transfer, but also depend on the reorienting and transfer rates, as

well as orientational *restrictions* of the donors. Hence, the rate of EET is influenced, since κ^2 depends on time if the transfer reorientations occur on similar time scales. To account for this an extended Förster theory was derived [8]. In this approach the excitation probability of the initially excited D within DD pairs reads;

$$\chi(t) = \frac{1}{2}\left\{\left\langle\left[1 + \exp\left(-2\int_0^t \omega(t')dt'\right)\right]\right\rangle\right\} F_{\mathrm{D}}(t)t) \tag{4}$$

Equation 4 is the solution to the *stochastic* master equation of energy migration within a DD pair, which was derived from the stochastic Liouville equation [9]. Notice in this context that $\{\langle \ldots \rangle\}$ denotes a *stochastic average*. At times $t \to 0$ Eq. 4 becomes equal to Eq. 3.

In general, mutual reorientations within a pair of donors usually change due to reorienting motions at each D-binding site, e.g. in a protein.

The fluorescence anisotropy $\{r(t)\}$ constructed from data recorded by depolarisation experiments is then composed of different contributions, as given below [10]:

$$r(t) = \frac{r(0)}{2}\left[\rho_{\mathrm{AA}}(t) + \rho_{\mathrm{BB}}(t) + \rho_{\mathrm{AB}}(t) + \rho_{\mathrm{BA}}(t)\right] exp\left(-t/\phi_{\mathrm{c,glob}}\right) \tag{5a}$$

As it stands, Eq. 5a also accounts for the overall global tumbling of the macromolecule ($\phi_{\mathrm{c,\ glob}}$), which often can be neglected [10]. The initial excitation probability of $\mathrm{D_A}$ and $\mathrm{D_B}$ is equal (= 1/2). The fluorescence anisotropy of each donor in the absence of EET is described by $\rho_{\mathrm{ii}}(t)$ (i = A or B). The contribution due to energy transfer from D_i to D_j is described by $\rho_{\mathrm{ij}}(t)$. Taken together the ρ-terms are:

$$\rho_{\mathrm{ii}}(t) = \left\langle P_2\left[\widehat{\mu}_i(0)\cdot\widehat{\mu}_i(t)\right]\frac{\chi(t)}{F_{\mathrm{D(t)}}}\right\rangle \; i = \mathrm{A,B} \tag{5b}$$

$$\rho_{\mathrm{ij}}(t) = \left\langle P_2\left[\widehat{\mu}_i(0)\cdot\widehat{\mu}_{\mathrm{j}}(t)\right]\frac{1-\chi(t)}{F_{\mathrm{D(t)}}}\right\rangle \; i,j = \mathrm{A,B\ where\ A} \neq \mathrm{B} \tag{5c}$$

$P_2\left[\widehat{\mu}_i(0)\cdot\widehat{\mu}_{\mathrm{j}}(t)\right]$ are second rank Legendre polynomials which correlate the mutual orientations of the electronic transition dipole moments at times of excitation ($t = 0$) and emission ($t = t$). For more details in applying the extended Förster theory the reader is kindly recommended to consider references [9] and [10], as well as papers cited therein.

2.2 *Analyses of EET Data of Donors in Spatial Distributions*

For systems composed of many randomly distributed donors undergoing energy migration one faces additional questions concerning the interpretation of

fluorescence depolarisation data. Firstly, how to account for the description of energy migration among several donors. This question involves the handling of many-donor interactions, but secondly also how to account for the influence of donor orientation rates and restrictions. The influence of translational motions in condensed media is usually negligible, since the fluorescence and energy transfer processes are much faster rates. However, by means of Monte Carlo (MC) simulations the description of these complicating circumstances can be overcome. For three-dimensional isotropic distributions of donors MC simulations have been compared with an analytical model previously derived [11]. It turns out that the agreement is very good at *reduced concentrations* of <2 [12]. The concept reduced concentration refers to the average number of interacting molecules (here donors) within a sphere defined by the Förster radius, R_0. In two-dimensional systems, the corresponding property refers to the average number of donors within a circle defined by R_0. For energy migration in two-dimensional *random* distributions, e.g. a model membrane or lipid bilayer, MC simulations [13] support a previously suggested model derived within the so-called two-particle approximation [14]. The two-particle approximation allows for deriving analytical equations for the time-dependent excitation probability of the *initially* excited donor $\{G^s(t)\}$. $G^s(t)$ depends on reduced concentrations (usually known) and certain mutual extreme orientations. For a lipid bilayer one needs to distinguish between inter- and intralayer donor energy migration. Within the Baumann-Fayer model [14] these contribute to the excitation probability of the initially excited donors yield as the joint probability:

$$G^s(t) = G^s_{\text{intra}}(t) G^s_{\text{inter}}(t) \tag{6}$$

A reasonable approach to modelling depolarisation experiments and to the fluorescence anisotropy reads:

$$r_{\text{DDEM}}(t) = G^s(t) r(t) \tag{7}$$

Here, $r(t)$ denotes the anisotropy obtained in the *absence* of energy migration, i.e. at low reduced concentrations.

In membranes composed of chemically different lipid species, the so-called rafts [15] may form. The rafts refer to regions comprising different lipid compositions. These regions mean non-uniform overall lipid distributions/compositions. From the studies of fluorophore-labelled lipids, MC analyses were adopted and indeed reveal heterogeneity in lipid membrane mixtures [16]. In a separate section of this book these aspects are further elaborated on.

2.3 *Analyses of EET Data Among Donors Within* Periodic *Spatial Distributions*

Some proteins form polymerised regular structures, i.e. arrangements with periodic spatial and orientation distributions of monomeric protein molecules. One important and well-known example is the muscle protein actin, which forms a helical structure, named F-actin [17] from monomeric actin, i.e. G-actin. For mixtures of mono-D-labelled monomers and wild type monomers, it is reasonable to assume a resulting non-covalent polymer with a statistically random distribution of labelled monomers. For different fractions of D-labelled monomers, one can investigate the influence of energy migration by means of fluorescence depolarisation experiments. Figure 2 displays data obtained for fractions of D-labelled G-actin ranging between 0.1 and 49 mol% [18]. As could be expected, the fluorescence anisotropy data reveal an increasing rate of energy migration with increasing D concentration. At the lowest concentration, however, there is an initial rapid relaxation of $r(t)$, which reaches a plateau region. The plateau region is compatible with the absence of energy migration, as well as the influence of F-actin and G-protein reorientations in the polymer on the timescale of fluorescence. Consequently, the anisotropy at <0.1 mol% represents F-actin containing *non-interacting* donor groups, where the initial relaxation can be ascribed to *local* reorientations of the donor group at its binding site. For a comparison, the anisotropy decays of donor labelled G-actin obtained at 277 and 293 K are also displayed in Fig. 2b. After a rapid initial relaxation a slower relaxation is observed which is compatible with the global orientation diffusion of the G-protein molecule.

The energy migration in the helical structure occurs among donors arranged within a repeated structural pattern, as is illustrated in Fig. 3. Every G-actin monomer exhibits a well-defined localisation with respect to its nearest neighbours. Because of the regular arrangement, it is therefore possible to use a limited number of unknown parameters to describe the relative monomer positions. These are defined in Fig. 3 and correspond to the distance from the helical axis (i.e. the C_∞-axis) to the labelled donor and that between labelled nearest D-groups along the C_∞-axis, denoted T_{xy} and T_z, respectively. The third parameter is the angle of rotation (θ) between nearest donor neighbours about the C_∞-axis. By means of MC simulations, it is possible to investigate possible migration paths and find the solutions that best fit to experimental data [18]. Notice, in common for all experimental data obtained on F-actin are the structural parameters (T_{xy}, T_z and θ) which should be invariant to the different degrees of labelling.

Data analyses are therefore suitable for a global analysis, i.e. all data are simultaneously fitted to the *same* model. The analyses require an efficient methodological approach, which enables the search of best-fit parameters in a multidimensional space. By using the so-called genetic algorithms this is possible [18, 19]. For further details, kindly consider reference [18] and papers cited therein.

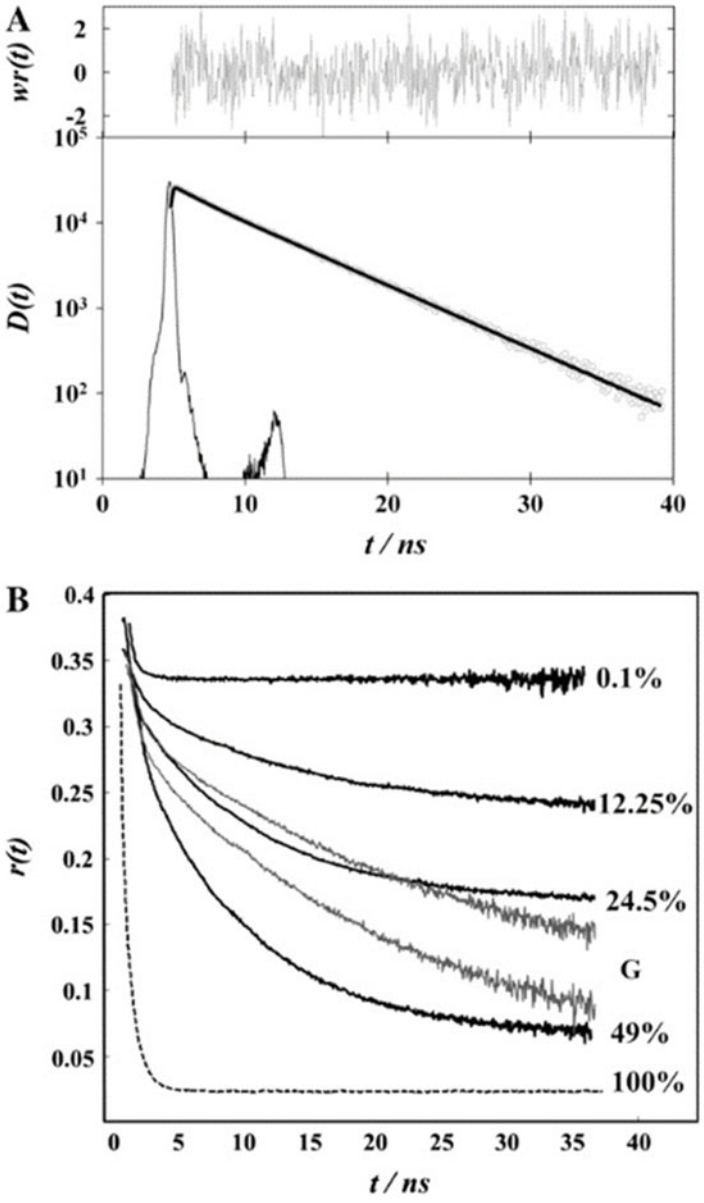

Fig. 2 Fluorescence depolarisation data obtained on fluorophore-labelled F-actin (BODIPY [18]). (**a**) The next most upper panel shows difference data {*D(t)*} obtained for a 0.1 mol% BODIPY-labelled F-actin. The best-fit obtained, i.e. weighted residuals {*wr(t)*} are displayed in the top panel. (**b**) A collection of fluorescence anisotropy {*r*(*t*)} data calculated from depolarisation experiments with various labelling degree of F-actin samples (in *black*). The % refer to different mole fractions of BODIPY-labelled F-actin at 277 K. The dashed curve was obtained from simulations using the parameters extracted from global analyses and when assuming 100 mol% labelling of F-actin. The two decay anisotropy curves (in *blue*) are data obtained for G-actin at 277 K (upper) and 293 K (lower). Reprinted with kind permission of Biophysical Journal

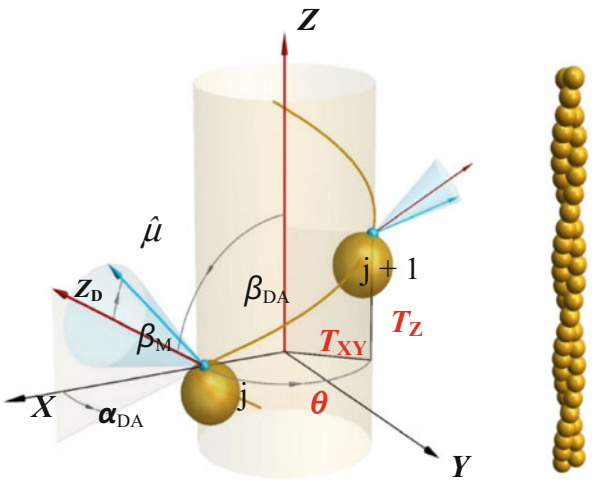

Fig. 3 Schematic showing the coordinate systems used to describe G-protein positions in regular structures forming helical, linear and ring-shaped aggregates. The Z_A axis coincides with the C_∞–axis of the aggregate, and T_{xy} denotes the distance from this axis to the position of a fluorescent group. The translational and rotational transformations between nearest protein neighbours are θ and T_z, respectively. The fluorophore undergoes local reorienting motions about an effective symmetry axis Z_D which transformed to the aggregate fixed frame by ($\propto_{DA}$, β_{DA})

3 Closing Comments

The aims of this chapter have been twofold; to provide a physical basis of electronic energy transfer, and to give a glimpse on the possibilities of using EET also as a *quantitative tool*, with focus on biomolecular applications on structure, function and dynamics. In this respect, I recall that few, if any luminescence quenching process, except for EET in the limit of weak coupling, can provide a quantitative connection between spectroscopic data and molecular properties.

Among several EET-applicants a crucial question concerns the orientation dependence of the coupling strength, i.e. the κ^2-factor, that can take values ranging between 0 (= i.e. forbidden EET) and 4. Another aspect deals with the influence of reorientation motions that can occur on the timescale of electronic coupling. In studies of systems with pairwise coupling, such as DA or DD labelled proteins, the handling of the κ^2-factor often needs to be carefully considered, preferably by means of independent experiments on donors and acceptors. The local motions and orientation restrictions of donors and acceptors can be determined from separate experiments on mono-labelled samples, which are then localised at adequate locations/positions in the structure investigated [10].

For DA systems with chromophores exhibiting *degenerate* transition dipoles in three dimensions, either of the D or the A group, the average κ^2-value will always be 2/3. Candidates of this kind are, for instance, complexes exhibiting charge-transfer transitions between metal ions and ligands of tetrahedral or higher symmetry.

Notice, it is sufficient if *one* of the components in a DA system fulfils this symmetry requirement. Hereby the rate of EET is solely dictated by the distance of separation (R).

A most powerful development for extending the applicability of EET on proteins would be to use "on-purpose designed" artificial fluorophoric amino acids. These would enable specific insertion at the level of expression of a protein, i.e. *site-specific mutagenesis*. The approach involves the development of a unique code for an *artificial* amino acid that corresponds to a specific codon, which enables insertion into the template sequence of the accessible primary sequence. In principle, any position in the protein structure is thereby replaceable by an artificial fluorophore. This approach would also solve the problem with specificity when labelling a protein with one donor and one acceptor. Furthermore, the methodology also makes it possible to label interior positions of a protein, which is tricky to perform.

Within the validity of Förster's mechanism EET experiments can be most informative for quantitative studies of structural *change,* e.g. in the presence of interacting components, such as substrates. This is a difficult task with NMR and X-ray methods, although these methods, no doubt, often can provide more detailed 3D structures. It should be emphasised that these established methods still are associated with severe limitations, not least concerning resolution and crystal quality. Thus, further developed/refined EET spectroscopy is a complementary tool, especially when insufficient structural information is unavailable by means of X-ray and NMR techniques.

References

1. Cario G (1922) Z Physik 10:185
2. Weiss J (1938) Nature 141:248
3. Weiss J (1939) Trans Faraday Soc 35:48
4. Förster T (1948) Ann Phys Berlin 2:55
5. Lakowicz JR (1999) Principles of fluorescence spectroscopy. Kluwer/Plenum, New York
6. Mikaelsson T, Ådén J, Wittung-Stafshede P, Johansson LB-Å (2014) Biophys J 107:401
7. Bergström F, Hägglöf P, Karolin J, Ny T, Johansson LB-Å (1999) PNAS 96:12477
8. Kubo R (1969) Stochastic processes in chemical physics. Advances in chemical physics, vol XVI, Shuler KE (ed). Wiley, New York
9. Johansson LB-Å, Edman P, Westlund P-O (1992) J Chem Phys 105:10896
10. Isaksson M, Hägglöf P, Håkansson P, Ny T, Johansson LB-Å (2007) PCCP 9:3914
11. Gouchanour CR, Andersen HC, Fayer MD (1979) J Chem Phys 70:4254
12. Engström S, Lindberg M, Johansson LB-Å (1988) J Chem Phys 89:204
13. Johansson LB-Å, Engström S, Lindberg M (1992) J Chem Phys 96:3844
14. Baumann J, Fayer MD (1986) J Chem Phys 85:4087
15. Hammond AT, Herbele FA, Baumgart T, Holowka D, Baird B, Feigenson GW (2005) PNAS USA 102:6320

16. Sachl R, Johansson LB-Å, Hof M (2012) Int J Mol Sci 13:16141
17. Lorentz M, Popp D, Holmes KC (1993) J Mol Biol 234:826
18. Marushchak D, Grenklo S, Johansson T, Karlsson R, Johansson LB-Å (2007) Biophys J 93: 3291
19. Charbonneau P (1995) Astrophys J Suppl Ser 101:309